the FEBS Journal

Balance of human choline kinase isoforms is critical for cell cycle regulation

Implications for the development of choline kinase-targeted cancer therapy

Jens Gruber[1,*,†], Wei Cun See Too[1,2,*], Mun Teng Wong[2], Arnon Lavie[3], Theresa McSorley[1] and Manfred Konrad[1]

1 Enzyme Biochemistry Research Group, Max-Planck-Institute for Biophysical Chemistry, Goettingen, Germany
2 School of Health Sciences, Universiti Sains Malaysia, Kubang Kerian, Kelantan, Malaysia
3 Department of Biochemistry and Molecular Genetics, University of Illinois at Chicago, Chicago, IL, USA

Keywords
anti-cancer strategy; cell cycle regulation; choline kinase; siRNA knockdown; subcellular localization

Correspondence
M. Konrad, PhD, Am Fassberg 11, D-37077 Goettingen, Germany
Fax: +49 551 2011074
Tel: +49 551 2011706
E-mail: mkonrad@gwdg.de
or
W. C. See Too, PhD, School of Health Sciences, Universiti Sains Malaysia, 16150 Kubang Kerian, Kelantan, Malaysia
Fax: +60 9 7677515
Tel: +60 9 7677537
E-mail: stweicun@kb.usm.my

*These authors contributed equally to this work

†Present address
German Primate Center, D-37077 Goettingen, Germany

(Received 20 December 2011, revised 24 February 2012, accepted 15 March 2012)

doi:10.1111/j.1742-4658.2012.08573.x

The enzyme choline kinase (CK), which catalyzes the phosphorylation of choline to phosphorylcholine in the presence of ATP, has an essential role in the biosynthesis of phosphatidylcholine, the major constituent of all mammalian cell membranes. CK is encoded by two separate genes expressing the three isoforms CKα1, CKα2 and CKβ that are active as homodimeric or heterodimeric species. Metabolic changes observed in various cancer cell lines and tumors have been associated with differential and marked up-regulation of the CKα genes, and specific inhibition of CKα activity has been proposed as a potential anti-cancer strategy. As a result, less attention has been given to CKβ and its interaction with CKα. With the aim of profiling the intracellular roles of CKα and CKβ, we used RNA interference (RNAi) as a molecular approach to down-regulate the expression of CK in HeLa cells. Individual and simultaneous RNAi-based silencing of the CK α and β isoforms was achieved using different combinations of knockdown strategies. Efficient knockdown was confirmed by immunodetection using our isoform-specific antibodies and by quantitative real-time PCR. Our analyses of the phenotypic consequences of CK depletion showed the expected lethal effect of CKα knockdown. However, CKβ- and CKα + CKβ-silenced cells had no aberrant phenotype. Therefore, our results support the hypothesis that the balance of the α and β isoforms is critical for cancer cell survival. The suppression of the cancer cell killing effect of CKα silencing by simultaneous knockdown of both isoforms implies that a more effective CK-based anti-cancer strategy can be achieved by reducing cross-reactivity with CKβ.

Abbreviations
AKT, serine/threonine-specific protein kinase, a downstream target of PI3K; CCl_4, carbon tetrachloride; CK, choline kinase; FITC, fluorescein isothiocyanate; GAPDH, glyceraldehyde-3-phosphate dehydrogenase; GL2, *Photinus pyralis* luciferase gene; MAPK, mitogen-activated protein kinase; PAH, polycyclic aromatic hydrocarbon; PCho, phosphocholine; PI3K, phosphatidylinositol 3-kinase; RNAi, RNA interference; siRNA, small interfering RNA, or silencing RNA; TUNEL, TdT-mediated biotin–dUTP nick-end labeling.

Introduction

Choline kinase (CK) (EC 2.7.1.32) catalyzes the phosphorylation of choline by ATP in the presence of Mg^{2+} to yield phosphocholine (PCho) and ADP [1]. This step commits choline to the so-called Kennedy or CDP-choline pathway for the biosynthesis of phosphatidylcholine, which represents the most abundant class of phospholipids in eukaryotic cells, constituting 40–60% of the phospholipid content in cell membranes [2]. In addition to forming the major structural component of the membrane bilayer, phosphatidylcholine also serves as a precursor for the production of lipid second messengers [3].

In mammals, including humans, CK is encoded by two separate genes named *ck-α* and *ck-β*. While *ck-β* codes for a single protein, CKβ (395 amino acids; NCBI accession number NP_005189), *ck-α* undergoes alternative splicing and is thus responsible for producing the two CK isoforms, α1 (439 amino acids; NCBI accession number NP_997634) and α2 (457 amino acids; NCBI accession number NP_001268), which differ by the presence of an 18-residue insert in α2 [4]. Human CKα1 and CKβ are 60% identical. Multiple genes, splice variants and studies showing differential regulation of multiple isoforms suggest that modulation of CK activity may occur predominantly at the level of gene expression [5]. However, *in vivo* and *in vitro* evidence for protein kinase-dependent phosphorylation of yeast and human CK indicates that the regulation of CK may also take place at the protein level [6–9]. Mammalian CK α and β isoforms are ubiquitously expressed in different tissues, as shown by northern and western blots [10]. One of the most intriguing characteristics of mammalian CK is its inducibility under various experimental conditions [1]. Polycyclic aromatic hydrocarbon (PAH) carcinogens caused long-lasting activation of rat and mouse hepatic CK [11,12], and the hepatotoxin carbon tetrachloride (CCl_4) also caused strong, but transient, induction of hepatic CK activity. The induction of hepatic CK by PAH and CCl_4 was found to be associated with increased expression of CK genes [11,13].

Interaction between the CK α and β isoforms to generate different combinations of dimeric complexes was first shown in mouse tissues [10]. More recently, physical interaction between the CK α and β isoforms to form different, enzymatically active, dimeric complexes was confirmed by the co-expression of mouse CKα and CKβ in COS-7 cells [4]. It was shown that about 60% of the total CK activity in mouse liver was attributable to the α/β heterodimeric species of the enzyme [10]. It has also been reported that the specific activity of α/α can be much higher than that of β/β [4]. Thus, the activity of CK in a given cell type could be regulated not only at the level of each isoform, but also through combination of the three isoforms (α1, α2 and β). However, the effect of interaction between different isoforms on the catalytic properties of dimeric (or higher oligomeric) CK still awaits further investigation. Recently, several essential domains and amino-acid residues important for the formation of active dimers have been identified by structural and mutational analyses of human and mouse CKα and CKβ [14,15].

Both CK and its reaction product, PCho, have been implicated in cell proliferation and transformation [16]. Generation of PCho was described as an essential event in growth factor-induced mitogenesis in fibroblasts [17,18] and PCho was found to cooperate with several mitogens [19]. Increased CK activity was reported in human breast cancer, and overexpression of CK is frequently observed in lung, prostate and colorectal cancers [20]. Increased levels of CKα were also detected in epithelial ovarian cancer [21] and in bladder carcinomas [22]. Furthermore, overexpression of several oncogenes (*ras*, *src* and *mos*) induces increased levels of CK and of PCho [23–26]. CK is activated by Ras proteins through a signaling pathway that involves two of their best-known effectors: Ral guanine nucleotide dissociation stimulator (Ral-GDS) and phosphatidylinositol 3-kinase (PI3K) [24]. CK, itself, was also shown to behave as an oncogene and was found to lie downstream of the RhoA GTPase-dependent signaling cascade [27]. Increased CK activity and elevated levels of PCho were found in human colon cancer [28] and in 1,2-dimethylhydrazine-induced rat colon cancer [29], as well as in human breast carcinomas [30]. Overexpression of CK was detected in a large panel of tumor-derived cell lines and in lung, prostate and colorectal cancers [31]. In addition, studies using NMR techniques have also shown elevated levels of PCho in various human tumoral tissues [32–34]. Elevation of the PCho content in breast cancer, detected by NMR spectroscopy, was consistent with the overexpression of CK as detected by microarray analyses [35]. These findings strongly support the role of CK in human cancer pathogenesis and suggest that the levels of CK and PCho could be used as tumor markers [36]. More recently, higher levels of CKα, but not of CKβ, were detected in multiple human breast cancer cell lines [37,38]. CKα was also considered as a potential prognostic factor for identifying nonsmall-cell lung cancer patients with a high risk of recurrence [39].

Specific inhibition of CK activity has been proposed as a promising anti-cancer strategy [26,40], and CK small-molecule inhibitors have been demonstrated to be potent anti-tumor drugs, both *in vitro* and *in vivo* [41,42]. Although the toxicity and side effects of CK inhibitors have largely been minimized [26], the long-term effect of such CK inhibitors on the tumor phenotype is still unknown [43]. As an alternative to enzyme inhibition, RNA interference (RNAi) offers a molecular approach to down-regulate the expression of specific target genes in mammalian cells. RNAi has also been used for dissecting the molecular basis of human diseases such as cancer [44]. Efforts to translate RNAi technologies into therapies for human diseases have surged in recent years, and RNAi-based drugs were found to have the potential of being more selective than traditional drugs [45]. RNAi knockdown of CKα in breast cancer cells was shown to reduce proliferation and to promote differentiation [43], and lentivirus-mediated CKα knockdown inhibited the growth of a human breast cancer xenograft [46]. Specific blockage of expression of the CKα isoform stimulated apoptosis [47] and selectively killed tumor cells, but not normal cells [48]. At the organismal level, the critical role of CK was shown in mice where CKα knockout resulted in early embryonic lethality [49], while CKβ knockout caused rostrocaudal muscular dystrophy [50]. Mutations in the gene encoding CKβ were also found in individuals with congenital muscular dystrophy [51].

The involvement of CKα in cancer pathogenesis has been well established, and drug inhibition of its activity or the knockdown of its gene expression, was proposed for potential cancer therapy [20,52]. However, the effect of simultaneous knockdown of both CK α and β isoforms on cancer cell growth has yet to be studied. Only recently was it shown that single or combined knockdown of CKα and CKβ reduced Akt(Ser473) phosphorylation to a similar level [53].

In this study, we explored a way of further profiling the intracellular roles of CKα and CKβ by individual and simultaneous RNAi knockdown of these two isoforms in HeLa cells. We designed siRNAs to induce the knockdown of human CK α and β isoforms and showed that single and double knockdowns can be achieved efficiently. Knockdown of CKα displayed a lethal phenotype; however, knockdown of CKβ resulted in no evident change in phenotype. Interestingly, the double knockdown appeared to reverse the lethality induced by the CKα single knockdown. Our results show the importance of interaction between CKα and CKβ, or their balanced expression levels, for cell cycle regulation. In addition, we observed both cytoplasmic and nuclear localization of CKα. These data may have implications for targeting CK as a potential anti-cancer strategy.

Results

Both CK α and β isoforms were successfully silenced, individually or simultaneously, in HeLa cells by siRNA transfection

The efficient silencing of CKα and CKβ in single- and double-knockdown experiments was confirmed by western blotting and quantitative RT-PCR. Cells were examined 24 and 48 h after transfection. Both single and double silencing resulted in the reduction of target isoforms below the levels detectable by western blotting (Fig. 1A). The results showed that silencing of CKα and CKβ had already taken place 24 h after transfection, even though the lethal phenotype of α-specific siRNA-transfected HeLa cells was only evident 48 h after transfection (see later). The real-time PCR results (Fig. 1B) showed that our siRNAs efficiently knocked down the targeted CK isoforms with efficiencies of 60–80%. The relative mRNA levels of CK isoforms under different siRNA treatments are shown in Fig. S1.

The highly specific CKα polyclonal antibody [38] was used to detect CKα by indirect immunofluorescence (Fig. 1C). The immunofluorescence data were consistent with the results obtained by immunoblotting and quantitative RT-PCR. Lower Rhodamine Red staining intensities in siCKα single knockdown and double siCKα + β double-knockdown cells, compared to cells treated with siGL2 or siCKβ, indicate efficient silencing of CKα. The CKβ siRNA-treated cells showed Rhodamine Red staining intensity that was very similar to cells treated with negative-control siRNA, indicating that the single silencing of CKβ did not affect the cellular level of CKα.

The basic goal of this study, namely the specific silencing of the individual human CK isoforms as well as the simultaneous knockdown of both genes, was achieved with proven efficiency. The phenotypic outcomes observed with different combinations of CKα- and CKβ-specific siRNA treatments (presented later) also provide additional support for the successful knockdown of both isoforms. The possibility of reduced CKα RNAi knockdown efficiency as a result of competition between CKα and CKβ siRNAs during co-transfection can be ruled out because western blotting and quantitative real-time PCR confirmed the drastically reduced level of CKα in double-knockdown cells.

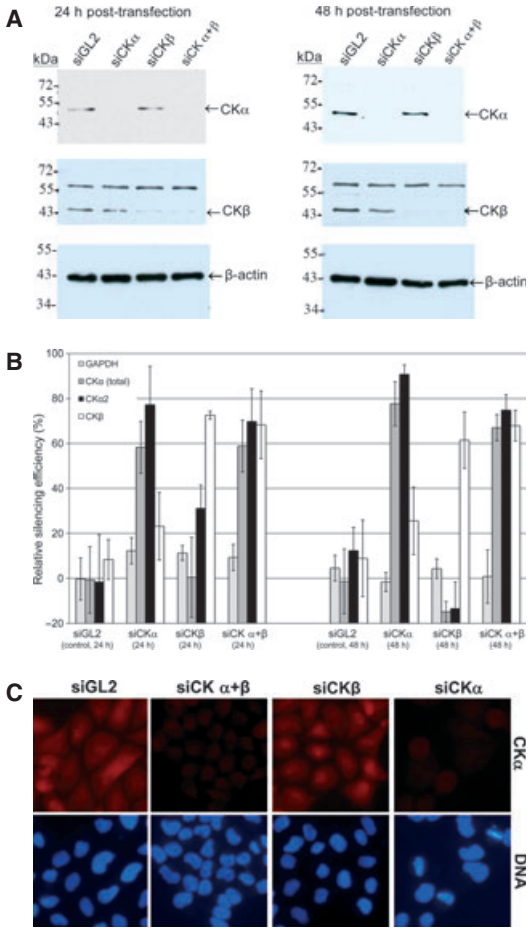

Fig. 1. Efficient silencing of human CK isoforms in HeLa cells. (A) Silencing of CKα and CKβ was confirmed by western blot analysis of HeLa cell lysates at 24 and 48 h post-transfection with siRNA. All lanes were loaded with 30 μg of cell lysate and confirmed by similar intensities of β-actin used as loading control. The band present between 55 and 72 kDa was nonspecifically stained with the CKβ antibody. (B) Silencing of total CKα, CKα2 and CKβ was confirmed by quantitative RT-PCR. The transcript levels were calculated and are shown as percentage knockdown relative to siGL2 knockdown, and normalized to a reference gene (GAPDH). (C) Immunofluorescence detection of CKα, 24 h after siRNA transfection, shows efficient silencing of CKα with single siCKα and double siCKα + siCKβ transfections. Transfections of siCKβ and siGL2 did not affect the cellular CKα levels.

CKα locates to the cytoplasm and also to the nucleoplasm, and its protein levels increase during mitosis

For a more quantitative view of the subcellular localization of CKα, we compared the protein levels in immunoblotted extracts of the nuclear and cytoplasmic fractions as well as in the total cell extract of HeLa cells using the CKα-specific antibody. In addition, we included extracts from mitotic cells in this assay. To exclude cross-contamination with nucleoplasmic or cytoplasmic components, the purity of extracts was confirmed by parallel probing of the blots with antibodies against cytoplasmic vimentin and nucleoplasmic lamin A/C.

Lamin A/C was detected in whole-cell extract, nucleoplasm and, to a lower extent, in the extract of mitotic cells, but not in cytoplasmic extract. The opposite was observed for cytoplasmic vimentin, which was present only in whole-cell and cytoplasmic extracts. However, CKα was found in all extracts tested (Fig. 2A). A higher level of CKα was detected in HeLa mitotic cell extract compared with whole-cell extract (Fig. 2A, lanes 1 and 4). These data indicate an unexpectedly high level of the enzyme within the nuclei of cells (compare lanes 2 and 3) and increased expression levels of CKα during mitosis (compare lanes 1 and 4). This finding was supported by separate indirect immunofluorescence microscopy in which a majority of cells displayed a higher level of CKα in the cytoplasm, but also a smaller fraction of cells (about 20%) with increased levels of CKα in their nuclei, as shown for a

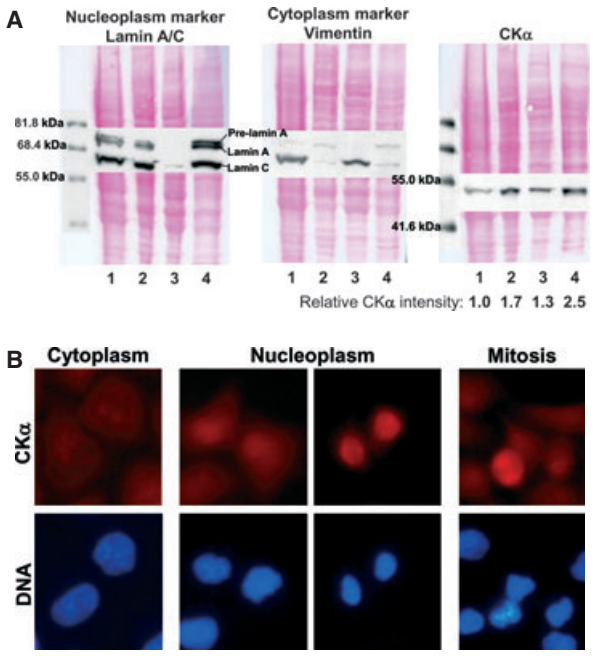

Fig. 2. Cellular localization of CKα. (A) Detection, by western blotting, of CKα in total cellular (lane 1), nucleoplasmic (lane 2), cytoplasmic (lane 3) and mitotic (lane 4) extracts of HeLa cells. Ponceau-S stain is shown in the background to confirm comparable protein loading. The relative intensities of CKα (normalized to the Ponceau-S staining intensity) are shown below the right panel. Intensity values were determined by ImageJ (http://rsbweb.nih.gov/ij/). (B) Immunofluorescence micrographs of untreated HeLa cells show the distribution of CKα in different cellular compartments.

population of HeLa cells in Fig. 2B. High levels of CKα were also present in mitotic cells (Fig. 2B, right panel), and staining with antibody showed a strong overlap of CKα with the mitotic spindle apparatus (see indirect immunofluorescence of mitotic spindle described below).

The nuclear localization of CKα was also supported by structure analysis using the sequence-based subcellular localization prediction program, PSORT II [54]. Both human CKα1 and CKα2 are predicted to localize in the nucleus, with a nuclear localization probability of 60.9% for CKα2 and of 52.2% for CKα1.

Individual silencing of CKα leads to a lethal phenotype and is rescued by simultaneous knockdown of CKα and CKβ

Silencing of human CK isoforms was originally aimed at investigating the phenotypic effect that might arise from elimination of these enzymes *in vivo*. At the same time, silencing of CKα and CKβ, separately and in combination, would answer the question of whether the two isoforms could complement each other's function, and whether knockdown of these two isoforms would result in a lethal phenotype, which would indicate that these two isoforms are essential enzymes for phosphatidylcholine synthesis.

Figure 3 shows the live cell imaging of HeLa cells treated with siRNAs targeting CKα and CKβ. The same adherent population of cells was located on CELLocate™ coverslips (Eppendorf) and photographed at 24- and 48-h time-points after transfection. The fate of a specific cell cluster could be followed during the entire course of the experiment. For single silencing of CKα, no apparent abnormal phenotype was detectable 24 h after transfection, and the cells appeared to multiply normally, with confluence similar to that of the negative control. However, a lethal phenotype was observed 48 h after transfection. Almost 90% of the total cell population died at this stage. Upon single silencing of CKβ, the cells showed no sign of abnormality up to 48 h after transfection. Surprisingly, however, double silencing of CKα and CKβ did not lead to lethality. Cells undergoing this combined silencing displayed a normal phenotype up to 48 h post-transfection. Thus, the siCKα single knockdown was lethal, although the level of CKβ protein was unchanged. On the other hand, the cells survived when the levels of both isoforms were reduced in double-knockdown experiments. Similar results were obtained with the MCF-7 cell line (Fig. S2). The lethal phenotype of single CKα knockdown was apparent at 72 h post-transfection, with more than 60% cells being dead

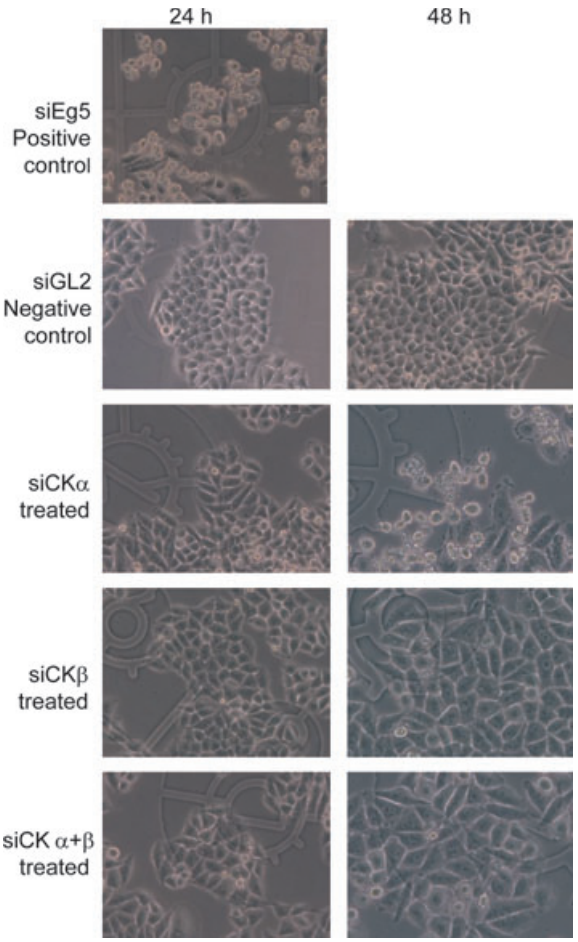

Fig. 3. Individual silencing of CKα leads to a lethal phenotype and is rescued by simultaneous knockdown of CKα and CKβ. Images of live cells at the same location (located by a Cellocate™ coverslip) were taken 24 and 48 h after transfection. Positive and negative control cells were transfected with Eg5 and GL2 luciferase siRNAs, respectively.

at this stage, whereas single CKβ and double CKα + CKβ knockdowns displayed a phenotype similar to that of the control. The onset of effects was observed ~ 24 h later than in HeLa cells. This is a result of the longer doubling times of MCF-7 cells (~ 36 h) [55] when compared with HeLa cells (~ 22 h). These results strongly suggest that the balance between CKα and CKβ dictates cell survival such that knockdown of CKβ reduces, or abolishes, the cell-killing effect of single CKα knockdown.

Only individual silencing of CKα leads to aberrant mitotic arrest and subsequent apoptosis

Indirect immunofluorescence (Fig. 4A) showed defects of the mitotic spindles of HeLa cells in the absence of

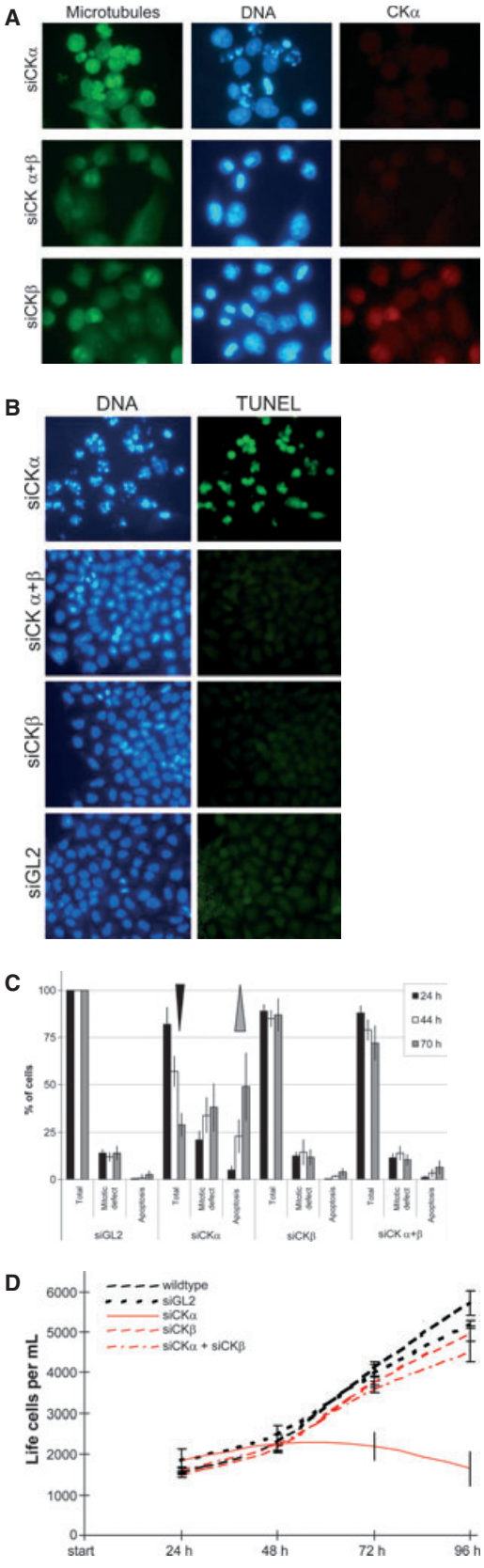

Fig. 4. Mitotic defects and apoptosis in HeLa cells after CKα silencing, but not after CKβ or CKα + CKβ double silencing. (A) Indirect immunofluorescence utilizing anti-α-tubulin IgG showed defects of the mitotic spindles in the absence of CKα (top panel), but not in CKα + CKβ double-silenced (middle panel) and CKβ-silenced (lower panel) cells. (B) The TUNEL assay, performed 72 h after siRNA transfection, showed that the single CKα-knockdown cell population was apoptotic, but no apoptotic cells were seen in control, siCKβ-silenced or CKα + CKβ double-silenced groups of cells. (C) Quantification of mitotic defects and apoptosis by cell counts after indirect immunofluorescence or the TUNEL assay. Decreased total cell counts (black triangle) and an increased number of apoptotic cells (grey triangle) were observed only for single siCKα-silenced cells. (D) Growth of HeLa cells after siRNA transfection was determined using a CASY cell count and analysis system over a period of 96 h. A significant decrease in the number of live cells was observed upon treatment with siCKα alone. Double-knockdown of both CKs affected cell growth only slightly.

CKα. Surprisingly, these abnormal spindle structures were not observed when both CKα and CKβ were silenced in parallel. Similarly, the single knockdown of CKβ also did not produce an aberrant mitotic phenotype. The siGL2 control showed normal mitotic spindles (Fig. S3, upper panels).

To further investigate the mechanism of cell death observed in single CKα silencing, a TdT-mediated biotin–dUTP nick-end labeling (TUNEL) assay was performed to identify cells with apoptosis-typical DNA double-strand breaks. An apoptotic effect was seen only in HeLa cells transfected with CKα-selective siRNA. The cells underwent aberrant mitotic arrest followed by apoptotic cell death in the gross majority of cells (> 75%) (Fig. 4B). Silencing of CKβ did not induce mitotic arrest and/or apoptosis. Also, simultaneous knockdown of both CKα and CKβ did not induce the effects observed for CKα silencing alone, and only a very small subpopulation (< 10%) of the cells displayed severe apoptotic effects.

A higher percentage of cells with mitotic defects and apoptosis was only observed for siCKα-treated HeLa cells 44 h after transfection (Fig. 4C). The level of mitotic defects and apoptosis for control, siCKβ and siCKα + siCKβ-transfected cells were similar throughout the experiment. As shown in Fig. 4D, the growth of siCKα-treated cells started to decline 48 h after transfection. Although the overall growth rates of the cells transfected with siCKβ alone, or with both siCKα and siCKβ, were slightly reduced when compared with wild-type (untreated) and control (siGL2-transfected), the general appearance of the cells upon transfection was normal.

Levels of CKα and CKβ play an essential role in progression through mitosis, but not in resting cells or during DNA replication

The significance of alteration of endogenous CKα and CKβ expression levels on the cell cycle was analyzed using synchronized HeLa cells. Cells arrested in the G0/G1 phase by serum starvation for 24–28 h were transfected with CKα, CKβ, or both, siRNAs (Fig. 5A). Apoptosis of these cells was not observed for up to 70 h after transfection (Fig. 5B). After release of the cells from serum starvation, by addition of fetal bovine serum to 10% v/v to the culture medium, the majority of cells re-entered cell cycle and died by apoptosis in the absence of CKα. Simultaneous silencing of CKα and CKβ in G0/G1-arrested cells did not induce apoptotic cell death after release from arrest in the G0/G1 phase. These cells properly completed their progression through mitosis. This indicates a critical importance of CKα expression levels relative to CKβ expression levels for progression through mitosis, whereas this imbalance does not play an essential role in resting cells.

To determine whether crucial effects arise during S phase (i.e. during DNA replication prior to mitotic entry), a double thymidine block was applied in combination with siRNA delivery. In this approach, DNA replication was inhibited by an excess of thymidine in the medium, or by addition of the DNA polymerase inhibitor, aphidicholin, resulting in a cell population stalled in S phase. As in the case of resting cells, no apparent differences between cells treated with control siRNA or siRNAs targeting CKα and/or CKβ were observed, indicating that the lack of CKα alone has no essential role in this phase of the cell cycle. After release from double thymidine-induced S-phase arrest, siCKα-treated cells displayed disordered microtubular structures, and cells that could not progress to metaphase showed apoptotic cell death (Fig. 6A). Double-silenced cells (siCKα + siCKβ), as well as cells transfected with siCKβ only, progressed successfully to mitosis. Silencing-linked apoptosis was not observed for either of these treatments. In both populations, ~ 50% of the cells showed synchronous transition to mitosis. The siGL2 control had a normal microtubular structure and no apoptosis after release from S-phase arrest (Fig. S3, lower panels). Figure 6B shows efficient knockdown of CKα by siCKα and siCKαβ in aphidicholin-induced S-phase arrest cells. Quantitative analysis of S-phase arrested cells (Fig. 6C) confirmed that CKα is not required during S phase but is essential for mitotic progress (metaphase or later). Few mitotic cells were seen during the double-thymidine block, and

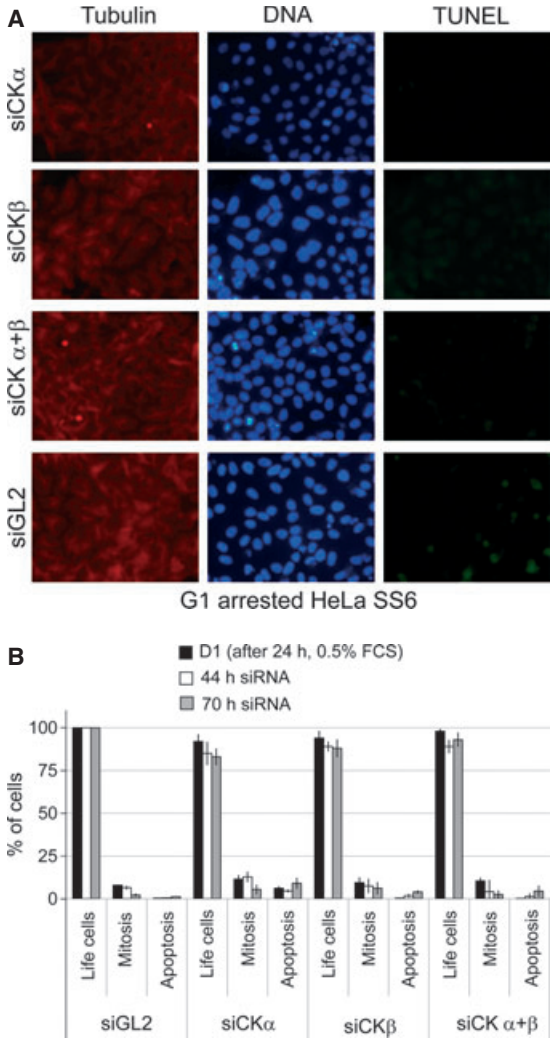

Fig. 5. Nonproliferating cells remain viable upon CKα silencing. (A) Fluorescence micrographs of G0/G1-arrested HeLa cells 44 h after siRNA transfection showed normal microtubular architecture and no apoptosis in the TUNEL assay. (B) Comparison of the relative numbers of viable cells and the proportion of cells with mitotic defects and apoptosis displayed efficient inhibition of cell proliferation by serum starvation. The number of cells with mitotic defects was comparable for all siRNA treatments, and no increase of apoptotic cells was observed after CKα silencing.

apoptosis was hardly observable in the blocking period. The absence of apoptosis in siCKα-transfected cells during S-phase arrest indicates that CKα is not essential in S phase. After release from the arrest, a majority of cells passed synchronously through mitosis, except for those cells transfected only with siCKα, which progressed directly into apoptotic cell death.

Microtubule-destabilizing agents are used to arrest cells at the mitotic entry point by inhibiting kinetochore attachment and thereby chromosome congression. In

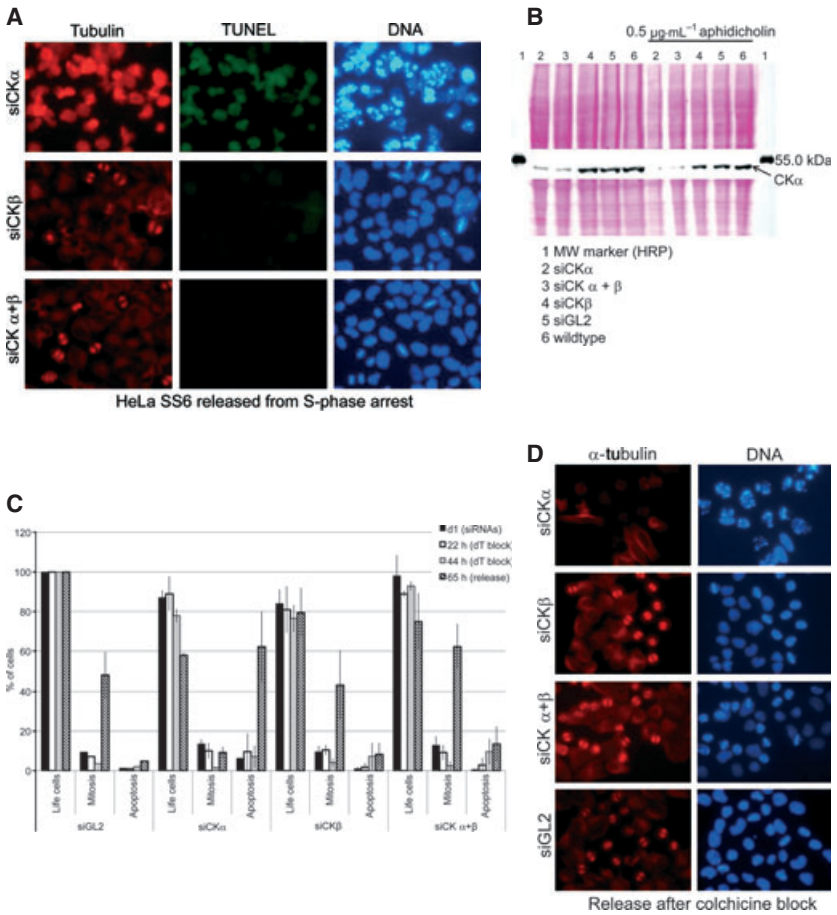

Fig. 6. Double-knockdown cells enter mitosis without showing disturbed chromosome congression seen in single-CKα knockdown cells. (A) Fluorescence micrographs of HeLa cells taken 8 h after release from double thymidine-induced S-phase arrest display high degrees of disordered microtubular structures and apoptosis in the siCKα-transfected population, but not in single-CKβ or double-CKα + CKβ silenced cells. (B) Western blot analysis of CKα in siRNA-transfected cells showed high knockdown efficiencies both in S-phase-arrested (by aphidicholin) cells and in proliferating cells. Ponceau-S stain is shown in the background to confirm comparable protein loading. (C) Quantitative analysis of cell counts demonstrates efficient S-phase arrest. Low percentages of mitotic and apoptotic cells were observed during the double-thymidine block. The absence of apoptosis in siCKα-transfected cells during S-phase arrest indicates that CKα is not essential in this phase. After release from the double- thymidine block (65 h), a majority of cells passed synchronously through mitosis, except for those cells transfected only with siCKα, which went directly into apoptotic cell death. (D) Fluorescence micrographs of HeLa cells taken after release from colchicine-induced mitotic arrest displayed a lethal phenotype for CKα-silenced cells. Control cells and those lacking both CKs progressed synchronously to the metaphase without major defects.

our study, we used colchicine to suppress mitotic spindle formation in CK-silenced cells. In contrast to the cells that were transfected with siCKβ alone, or with both siCKα and siCKβ, the CKα-knockdown cells were not capable of establishing proper mitotic spindle formation after release from mitotic entry arrest (Fig. 6D). Immediately after release from colchicine treatment, control cells and those lacking both CKs synchronously progressed to the metaphase without major defects. CKα-deficient cells suffered from severe mitotic defects and directly underwent apoptotic cell death, as shown by α-tubulin staining and by staining chromatin with Hoechst 33342. Double-knockdown of CKα and CKβ did not result in highly disordered spindle microtubules, inadequate kinetochore attachment and severely disturbed chromosome congression, as seen in the case of single CKα knockdown (Fig. 6D).

Discussion

Systematic knockdown of human CK isoforms by the RNAi technique is an attractive way to analyze the role of different isoforms, as well as to probe for any

unexpected functions of these enzymes. In this study, we have confirmed, by immunodetection and quantitative RT-PCR, that siRNAs efficiently silence CKα and CKβ in both single- and double-knockdown experimental conditions. Our work demonstrates the potent apoptotic effect displayed by the CKα-specific siRNA. More importantly, we found that simultaneous knockdown of CKα and CKβ did not enhance the lethal effect of single knockdown of CKα, but rather prevented cell killing. Our results are in accordance with previous reports on reduced proliferation of malignant cell lines by specific CKα knockdown [43,46,48,56]. Large-scale RNAi knockdown screening, aiming to identify human kinases that regulate cell survival and apoptosis, also showed that single knockdown of human CKα increased apoptosis by about twofold [47]. Owing to the relevance of CKα in human carcinogenesis, the role of CKβ has been largely neglected. Only recently was RNAi knockdown of CKβ plus CKα performed to investigate the effect of CK knockdown on Akt protein kinase phosphorylation [53]. However, the authors did not analyze the effect of double knockdown on cell proliferation.

Mammalian CKs are thought to be cytoplasmic enzymes [1]. Yet, the nuclear localization of CKα, as observed in this study, supports the notion that the presence of CDP-choline pathway enzymes, including CK in the nucleus, is required for the synthesis of endonuclear phosphatidylcholine, which, in turn, is an important source of diacylglycerol for nuclear lipid signaling [57–59].

Inhibition of, or defects in, the CDP-choline pathway are known to result in cell cycle arrest and apoptosis [60,61]. The same phenotypes were observed in the case of our single CKα knockdown. In this report, we highlight the absence of apoptosis when both CK isoforms were knocked down in proliferating HeLa cells. Double-knockdown cells were able to enter mitosis without showing disrupted chromosome congression, as seen in the single CKα knockdown cells. According to our observation, we propose that a higher level of CKα compared with CKβ is required for the proliferation of cancer cells. Under single CKα knockdown, the level of CKβ exceeds that of CKα, which suppressed cell growth and induced apoptosis. However, under double knockdown of CKα and CKβ with similar knockdown efficiencies, the level of CKα became higher than the level of CKβ (as a result of its higher initial level in cancer cells), thus fulfilling the requirement for cell proliferation. Our results clearly show that double knockdown of CKα and CKβ can rescue the cells from apoptotic cell death in single CKα-silenced cells. Therefore, exclusive silencing of CKα is critical when using RNAi as a potential novel anti-cancer approach. More importantly, if the effects of CKα and CKβ knockdown are related to the activities of these enzymes, this would imply that specific inhibition of CKα alone is the best way to induce apoptosis. Therefore, we believe that inhibition of CK activity as an anti-cancer strategy must focus on the specific inhibition of CKα, without affecting the activity of CKβ, in order to induce maximum apoptosis in the target cancer cells.

Furthermore, the results of CKα and CKβ silencing experiments performed in this work suggest other unexpected and essential roles of the interaction between these enzymes in the cell cycle, particularly in the progression to the mitotic phase. The apoptotic effect seen in cells treated with single CKα knockdown cannot be explained by the simple loss-of-function hypothesis because cells treated with double CKα and CKβ knockdown displayed a viable phenotype. According to Yalcin *et al.* [62], selective RNAi inhibition of CKα decreases the steady-state concentrations of phosphatidylcholine and phosphatidic acid, attenuates mitogen-activated protein kinase (MAPK) and PI3K/serine/threonine-specific protein kinase (AKT) survival pathways, and markedly reduces the survival of HeLa cells. In our study, the simultaneous depletion of both CKα and CKβ might re-activate MAPK and PI3K/AKT pathways through the production of phosphatidic acid, the key activator of these two signaling pathways. Overexpression of CKα and CKβ in HEK293T cells revealed a distinct metabolic role of the two isoforms *in vivo* and showed that both were regulated differently by Ras and Rho GTPases [52]. Our results suggest that CKα and CKβ are components of different signaling pathways that might interact to determine cell survival and proliferation.

In summary, this work has shown efficient siRNA-mediated individual and simultaneous knockdown of human CKα and CKβ isoforms in HeLa and MCF-7 cells. Silencing of CKα alone inhibited progression of cells into the mitotic phase and subsequently resulted in apoptosis. Remarkably, double knockdown of both CKα and CKβ isoforms rescued the cells from undergoing apoptosis. Our work implies that RNAi-based silencing of CK expression can be used as a potential anti-cancer strategy by emphasizing the specific knockdown or inhibition of the CKα isoform to induce apoptosis.

Experimental procedures

Cell lines and cell cycle synchronization

Human cervix epithelial carcinoma cells, HeLa SS6, and human breast adenocarcinoma cells, MCF-7, were maintained in Dulbecco's modified Eagle's medium (DMEM) with 10% (v/v) fetal calf serum and supplemented with

100 U·mL^{-1} of penicillin/streptomycin antibiotic mix (Sigma, St Louis, MO, USA). For G0/G1 arrest, cells were cultured under serum-starvation conditions (0.25% fetal calf serum in culture medium) for 24 h prior to siRNA transfection and continued to starve until final examination of the samples. S-phase arrest was induced by a double-thymidine block, by adding 0.2 mM thymidine to the culture medium for 10 h to block DNA replication. The medium was replaced with standard culture medium for 3 h and subsequently supplemented with 0.2 mM thymidine, again for 10 h prior to transfection. Alternatively, S-phase arrest was forced by adding 0.5 μg·mL^{-1} of aphidicholin to the culture medium for 16 h to inhibit polymerase activities. Mitotic entry arrest was induced by supplementing the culture medium with 7.5 μg·mL^{-1} of microtubule-destabilizing colchicine for 60 min shortly after siRNA transfection. Release from mitotic or S-phase arrests was performed by removing the medium, washing the cells twice with prewarmed sterile NaCl/P_i and adding fresh standard culture medium. To determine the percentage of mitotic and apoptotic cells, 1000–1500 cells per probe were counted manually, and the number of mitotic or apoptotic cells in the same population was determined.

Cell extracts and antibodies

SDS/PAGE and western blotting were performed according to standard protocols. HeLa cell lysates were prepared by suspending the cells in lysis buffer containing 10 mM K_2HPO_4, 150 mM NaCl, 5 mM EDTA, 5 mM EGTA, 1% Triton X-100, 0.2% deoxycholate and protease inhibitor cocktail (Roche, Mannheim, Germany), pH 7.4. The cell suspension was homogenized and cell debris was precipitated by centrifugation. The protein concentration of the supernatant was determined by the dye-binding method [63]. Upon immunoblotting, bands were detected using ECL (Amersham Pharmacia, Piscataway, NJ, USA). Affinity-purified horseradish peroxidase-conjugated goat anti-mouse and goat anti-rabbit immunoglobulins were from Dako (Hamburg, Germany). Extracts of cytoplasm and nucleoplasm from HeLa cells were kindly provided by R. Luehrmann (MPIbpc, Goettingen, Germany). Polyclonal rabbit anti-CKα serum was produced as described previously [38]. Polyclonal anti-CKβ IgG was produced by immunizing rabbit with highly purified recombinant human CKβ protein [38] and the immunoglobulin was obtained by affinity purification. Monoclonal mouse anti-(β-actin) (clone AC-15) IgG was from Abcam. Monoclonal antibodies recognizing vimentin (clone V9; 64) and lamin A/C (clone 636.23; [65]) were kindly provided by M. Osborn (MPIbpc).

Indirect immunofluorescence microscopy

Immunofluorescence staining and microscopy were performed according to standard protocols [66]. Cells were fixed either in −20 °C methanol for 10 min or at room temperature in 3.7% paraformaldehyde for 30 min, followed by permeabilization in 0.2% Triton X-100 in NaCl/P_i for 5 min. Subsequently, 30 μL of primary antibody per coverslip were applied evenly onto the cells and incubated at 37 °C for 1 h. After washing three times in NaCl/P_i, 30 μL of secondary antibody was spread evenly on the cells. The coverslips were incubated for 45 min at 37 °C followed by three washes in NaCl/P_i. Monoclonal anti-(α-tubulin) was kindly provided by M. Osborn (MPIbpc). Fluorescein isothiocyanate (FITC)- or rhodamine-conjugated goat anti-mouse and rhodamine-conjugated goat anti-rabbit Igs were from Dako. DNA was visualized by staining with Hoechst 33342 dye.

TUNEL assay

For detection of apoptosis, a TUNEL test (*In Situ* Cell Death Detection Kit; Roche) was performed, as described previously [66]. Transfected cells grown for 60 h were fixed in −20 °C methanol for 6 min and treated with NaCl/P_i containing 0.1% Triton X-100 and 0.1% sodium citrate on ice for 2 min. Free 3′ ends of fragmented DNA were enzymatically labeled with FITC-tagged dNTPs using terminal deoxynucleotidyl transferase (TdT). Labeled DNA fragments were monitored by fluorescence microscopy.

Growth rate determination

The examination of growth rates after transfection, and the detection of dead cells in the cell suspension were carried out using the Cell Counter and Analysis System (CASY® Model TT; Schärfe System, Munich, Germany). For CASY measurements, medium from one well of a six-well plate containing siRNA-transfected cells was discarded and the cells were trypsinized with 0.25 mL of trypsin/EDTA solution. After 1 min of incubation at 37 °C, the trypsin was quenched by the addition of 1.5 mL of DMEM + 10% FCS. Then, 100 μL of this solution was mixed with 10 mL of CASY®ton (Schärfe System GmbH, Reutlingen, Germany) isotonic dilution liquid and used directly for cell counting. When the cell numbers were too high, the solution was diluted further with CASY®ton.

Design of siRNAs and transfection

The siCKα probe was designed to target both α1 and α2 isoforms of CK, while siCKβ was CKβ specific. The following siRNA sequences are given in 5′ to 3′ orientation, and the position numbers are relative to the first nucleotide of the ORF.

siCKα (α2 position numbers 636–654; the sequence is also shared with α1 at position numbers 582–600):
CGAUUAGAUACUGAAGAA
siCKβ (position numbers 503–521):
CCACGAAGAUGGCGCAAUU

Noncognate siGL2, targeting firefly luciferase (position numbers 153–175): CACGUACGCGGAAUACUUCGAAA
siEg5 motor protein (position numbers 1547–1569): AACUGGAUCGUAAGAAGGCAGUU

Transfection of siRNA with oligofectamine (Invitrogen) was performed as described previously [66]. The cells were seeded in 24-well plates 20 h prior to transfection, and for microscopic analysis, they were grown on glass coverslips. The oligofectamine–siRNA mixture was added to a final concentration of 100 nM siRNAs in the culture medium.

Quantitative real time-PCR

The silencing of CKα and CKβ expression was also determined by quantitative RT-PCR. Total RNA was isolated using the RNeasy Mini kit (Qiagen, Hilden, Germany). Total RNA from control and different siRNA-treated cells was reverse-transcribed using the Omniscript reverse transcription kit (Qiagen). The reaction consisted of 1.0 μL of 10 × Omniscript RT buffer, 1.0 μg of total RNA and distilled deionized water to a final volume of 7.5 μL. The mixture was heated to 65 °C for 5 min to denature RNA, 1.0 μM of oligo-dT primer (Stratagene, La Jolla, CA, USA) was added and the reaction was incubated at room temperature for 10 min before the addition of 2.0 units of Omniscript reverse transcriptase and dNTPs to a final concentration of 0.5 mM. The reaction was incubated at 37 °C for 2 h.

The cDNAs generated were subjected to quantitative real time-PCR utilizing SYBR Green chemistry (Applied Biosystems, Carlsbad, CA, USA) on an ABI7500 cycler. Primer sets for total CKs α or specific for CKα2 as well as for CKβ were used, and glyceraldehyde-3-phosphate dehydrogenase (GAPDH) served as the normalization target. Quantitative RT-PCR (qRT-PCR) was performed, according to the manufacturer's guidelines, for 35 cycles in 20-μl reactions with 20 ng of cDNA template and 200 nM primer. Analysis was based on normalized values and calculation of $\Delta\Delta C_T$ values relative to the cDNA of control cells [67]. DDC_T is defined as the difference between the DC_T threshold cycle values of each siRNA treatment and the DC_T value of siGL2 (control). Primer sequences for CK isoform-specific sets are given as follows (each in 5′ to 3′orientation). Total CKα forward: tcagagcaaacatccggaagt (position numbers 1031–1051 in the CKα1 cDNA sequence or position numbers 1085–1105 in the CKα2 cDNA sequence); reverse: ggcgtagtccatgtacccaaat (position numbers 1248–1269 in the CKα1 cDNA sequence or position numbers 1302–1323 in the CKα2 cDNA sequence). CKα2 forward: ggccttagcaacatgctgttc (position numbers 355–375 in both CKα1 and CKα2 cDNA sequences); reverse: agcttgttcagagccctctt (located in the cDNA sequence unique to CKα2, position numbers 476–495). CKβ forward: atgttcgccatacttgcgga (position numbers 364–383 in the CKβ cDNA sequence); reverse: aattgcgccatcttcgtgg (position numbers 503–521 in the CKβ cDNA sequence).

Primers for the GAPDH reference gene were from Hs_GAPDH_1_SG QuantiTect Primer Assay kit (Qiagen). All data are representative of triplicate experiments.

Acknowledgements

W.C.S.T. was supported by the Academic Staff Training Scheme of Universiti Sains Malaysia. J.G. and T.M. were supported by the German Research Foundation (DFG). M.T.W. was supported by Universiti Sains Malaysia Postgraduate Fellowship. This work was partly supported by Universiti Sains Malaysia RU grant (1001/PPSK/813034).

References

1 Ishidate K (1997) Choline/ethanolamine kinase from mammalian tissues. *Biochim Biophys Acta* **1348**, 70–78.
2 Kent C (1990) Regulation of phosphatidylcholine biosynthesis. *Prog Lipid Res* **29**, 87–105.
3 Exton JH (2000) Phospholipase D. *Ann N Y Acad Sci* **905**, 61–68.
4 Aoyama C, Liao H & Ishidate K (2004) Structure and function of choline kinase isoforms in mammalian cells. *Prog Lipid Res* **43**, 266–281.
5 Gee P & Kent C (2003) Multiple isoforms of choline kinase from Caenorhabditis elegans: cloning, expression, purification, and characterization. *Biochim Biophys Acta* **1648**, 33–42.
6 Choi MG, Kurnov V, Kersting MC, Sreenivas A & Carman GM (2005) Phosphorylation of the yeast choline kinase by protein kinase C. Identification of Ser25 and Ser30 as major sites of phosphorylation. *J Biol Chem* **280**, 26105–26112.
7 Kim KH & Carman GM (1999) Phosphorylation and regulation of choline kinase from *Saccharomyces cerevisiae* by protein kinase A. *J Biol Chem* **274**, 9531–9538.
8 Yu Y, Sreenivas A, Ostrander DB & Carman GM (2002) Phosphorylation of *Saccharomyces cerevisiae* choline kinase on Ser30 and Ser85 by protein kinase A regulates phosphatidylcholine synthesis by the CDP-choline pathway. *J Biol Chem* **277**, 34978–34986.
9 Miyake T & Parsons SJ (2011) Functional interactions between Choline kinase alpha, epidermal growth factor receptor and c-Src in breast cancer cell proliferation. *Oncogene* **31**, 1431–1441.
10 Aoyama C, Ohtani A & Ishidate K (2002) Expression and characterization of the active molecular forms of choline/ethanolamine kinase-alpha and -beta in mouse tissues, including carbon tetrachloride-induced liver. *Biochem J* **363**, 777–784.
11 Ishidate K, Tsuruoka M & Nakazawa Y (1980) Induction of choline kinase by polycyclic aromatic

hydrocarbon carcinogens in rat liver. *Biochem Biophys Res Commun* **96**, 946–952.
12 Paulson BK, Porter TJ & Kent C (1989) The effect of polycyclic aromatic hydrocarbons on choline kinase activity in mouse hepatoma cells. *Biochim Biophys Acta* **1004**, 274–277.
13 Ishidate K, Enosawa S & Nakazawa Y (1983) Actinomycin D-sensitive induction of choline kinase by carbon tetrachloride intoxication in rat liver. *Biochem Biophys Res Commun* **111**, 683–689.
14 Liao H, Aoyama C, Ishidate K & Teraoka H (2006) Deletion and alanine mutation analyses for the formation of active homo- or hetero-dimer complexes of mouse choline kinase-alpha and -beta. *Biochim Biophys Acta* **1761**, 111–120.
15 Malito E, Sekulic N, Too WC, Konrad M & Lavie A (2006) Elucidation of human choline kinase crystal structures in complex with the products ADP or phosphocholine. *J Mol Biol* **364**, 136–151.
16 Glunde K, Bhujwalla ZM & Ronen SM (2011) Choline metabolism in malignant transformation. *Nat Rev Cancer* **11**, 835–848.
17 Cuadrado A, Carnero A, Dolfi F, Jimenez B & Lacal JC (1993) Phosphorylcholine: a novel second messenger essential for mitogenic activity of growth factors. *Oncogene* **8**, 2959–2968.
18 Jimenez B, del Peso L, Montaner S, Esteve P & Lacal JC (1995) Generation of phosphorylcholine as an essential event in the activation of Raf-1 and MAP-kinases in growth factors-induced mitogenic stimulation. *J Cell Biochem* **57**, 141–149.
19 Chung T, Crilly KS, Anderson WH, Mukherjee JJ & Kiss Z (1997) ATP-dependent choline phosphate-induced mitogenesis in fibroblasts involves activation of pp70 S6 kinase and phosphatidylinositol 3′-kinase through an extracellular site. Synergistic mitogenic effects of choline phosphate and sphingosine 1-phosphate. *J Biol Chem* **272**, 3064–3072.
20 Gallego-Ortega D, Gomez del Pulgar T, Valdes-Mora F, Cebrian A & Lacal JC (2011) Involvement of human choline kinase alpha and beta in carcinogenesis: a different role in lipid metabolism and biological functions. *Adv Enzyme Regul* **51**, 183–194.
21 Iorio E, Ricci A, Bagnoli M, Pisanu ME, Castellano G, Di Vito M, Venturini E, Glunde K, Bhujwalla ZM, Mezzanzanica D *et al*. (2010) Activation of phosphatidylcholine cycle enzymes in human epithelial ovarian cancer cells. *Cancer Res* **70**, 2126–2135.
22 Hernando E, Sarmentero-Estrada J, Koppie T, Belda-Iniesta C, Ramirez de Molina V, Cejas P, Ozu C, Le C, Sanchez JJ, Gonzalez-Baron M *et al*. (2009) A critical role for choline kinase-alpha in the aggressiveness of bladder carcinomas. *Oncogene* **28**, 2425–2435.
23 Ramirez de Molina A, Rodriguez-Gonzalez A, Penalva V, Lucas L & Lacal JC (2001) Inhibition of ChoK is an efficient antitumor strategy for Harvey-, Kirsten-, and N-ras-transformed cells. *Biochem Biophys Res Commun* **285**, 873–879.
24 Ramirez de Molina A, Penalva V, Lucas L & Lacal JC (2002) Regulation of choline kinase activity by Ras proteins involves Ral-GDS and PI3K. *Oncogene* **21**, 937–946.
25 Ratnam S & Kent C (1995) Early increase in choline kinase activity upon induction of the H-ras oncogene in mouse fibroblast cell lines. *Arch Biochem Biophys* **323**, 313–322.
26 Hernandez-Alcoceba R, Saniger L, Campos J, Nunez MC, Khaless F, Gallo MA, Espinosa A & Lacal JC (1997) Choline kinase inhibitors as a novel approach for antiproliferative drug design. *Oncogene* **15**, 2289–2301.
27 Ramirez de Molina A, Gallego-Ortega D, Sarmentero J, Banez-Coronel M, Martin-Cantalejo Y & Lacal JC (2005) Choline kinase is a novel oncogene that potentiates RhoA-induced carcinogenesis. *Cancer Res* **65**, 5647–5653.
28 Nakagami K, Uchida T, Ohwada S, Koibuchi Y, Suda Y, Sekine T & Morishita Y (1999) Increased choline kinase activity and elevated phosphocholine levels in human colon cancer. *Jpn J Cancer Res* **90**, 419–424.
29 Nakagami K, Uchida T, Ohwada S, Koibuchi Y & Morishita Y (1999) Increased choline kinase activity in 1,2-dimethylhydrazine-induced rat colon cancer. *Jpn J Cancer Res* **90**, 1212–1217.
30 Ramirez de Molina A, Gutierrez R, Ramos MA, Silva JM, Silva J, Bonilla F, Sanchez JJ & Lacal JC (2002) Increased choline kinase activity in human breast carcinomas: clinical evidence for a potential novel antitumor strategy. *Oncogene* **21**, 4317–4322.
31 Ramirez de Molina A, Rodriguez-Gonzalez A, Gutierrez R, Martinez-Pineiro L, Sanchez J, Bonilla F, Rosell R & Lacal J (2002) Overexpression of choline kinase is a frequent feature in human tumor-derived cell lines and in lung, prostate, and colorectal human cancers. *Biochem Biophys Res Commun* **296**, 580–583.
32 Bhakoo KK, Williams IT, Williams SR, Gadian DG & Noble MD (1996) Proton nuclear magnetic resonance spectroscopy of primary cells derived from nervous tissue. *J Neurochem* **66**, 1254–1263.
33 Podo F (1999) Tumour phospholipid metabolism. *NMR Biomed* **12**, 413–439.
34 Ronen SM, Jackson LE, Beloueche M & Leach MO (2001) Magnetic resonance detects changes in phosphocholine associated with Ras activation and inhibition in NIH 3T3 cells. *Br J Cancer* **84**, 691–696.
35 Glunde K, Jie C & Bhujwalla ZM (2004) Molecular causes of the aberrant choline phospholipid metabolism in breast cancer. *Cancer Res* **64**, 4270–4276.
36 Rodriguez-Gonzalez A, Ramirez de Molina A, Benitez-Rajal J & Lacal JC (2003) Phospholipase D and choline

kinase: their role in cancer development and their potential as drug targets. *Prog Cell Cycle Res* **5**, 191–201.
37 Eliyahu G, Kreizman T & Degani H (2007) Phosphocholine as a biomarker of breast cancer: molecular and biochemical studies. *Int J Cancer* **120**, 1721–1730.
38 See Too WC, Wong MT, Few LL & Konrad M (2010) Highly specific antibodies for co-detection of human choline kinase alpha1 and alpha2 isoforms. *PLoS One* **5**, e12999.
39 Ramirez de Molina A, Sarmentero-Estrada J, Belda-Iniesta C, Taron M, Ramirez de Molina V, Cejas P, Skrzypski M, Gallego-Ortega D, de Castro J, Casado E *et al*. (2007) Expression of choline kinase alpha to predict outcome in patients with early-stage non-small-cell lung cancer: a retrospective study. *Lancet Oncol* **8**, 889–897.
40 Lacal JC (2001) Choline kinase: a novel target for antitumor drugs. *IDrugs* **4**, 419–426.
41 Rodriguez-Gonzalez A, de Molina AR, Fernandez F, Ramos MA, Nunez Mdel C, Campos J & Lacal JC (2003) Inhibition of choline kinase as a specific cytotoxic strategy in oncogene-transformed cells. *Oncogene* **22**, 8803–8812.
42 Rodriguez-Gonzalez A, Ramirez de Molina A, Banez-Coronel M, Megias D & Lacal JC (2005) Inhibition of choline kinase renders a highly selective cytotoxic effect in tumour cells through a mitochondrial independent mechanism. *Int J Oncol* **26**, 999–1008.
43 Glunde K, Raman V, Mori N & Bhujwalla ZM (2005) RNA interference-mediated choline kinase suppression in breast cancer cells induces differentiation and reduces proliferation. *Cancer Res* **65**, 11034–11043.
44 Willingham AT, Deveraux QL, Hampton GM & Aza-Blanc P (2004) RNAi and HTS: exploring cancer by systematic loss-of-function. *Oncogene* **23**, 8392–8400.
45 Mahanthappa N (2005) Translating RNA interference into therapies for human disease. *Pharmacogenomics* **6**, 879–883.
46 Krishnamachary B, Glunde K, Wildes F, Mori N, Takagi T, Raman V & Bhujwalla ZM (2009) Noninvasive detection of lentiviral-mediated choline kinase targeting in a human breast cancer xenograft. *Cancer Res* **69**, 3464–3471.
47 MacKeigan JP, Murphy LO & Blenis J (2005) Sensitized RNAi screen of human kinases and phosphatases identifies new regulators of apoptosis and chemoresistance. *Nat Cell Biol* **7**, 591–600.
48 Banez-Coronel M, de Molina AR, Rodriguez-Gonzalez A, Sarmentero J, Ramos MA, Garcia-Cabezas MA, Garcia-Oroz L & Lacal JC (2008) Choline kinase alpha depletion selectively kills tumoral cells. *Curr Cancer Drug Targets* **8**, 709–719.
49 Wu G, Aoyama C, Young SG & Vance DE (2008) Early embryonic lethality caused by disruption of the gene for choline kinase alpha, the first enzyme in phosphatidylcholine biosynthesis. *J Biol Chem* **283**, 1456–1462.
50 Sher RB, Aoyama C, Huebsch KA, Ji S, Kerner J, Yang Y, Frankel WN, Hoppel CL, Wood PA, Vance DE *et al*. (2006) A rostrocaudal muscular dystrophy caused by a defect in choline kinase beta, the first enzyme in phosphatidylcholine biosynthesis. *J Biol Chem* **281**, 4938–4948.
51 Mitsuhashi S, Hatakeyama H, Karahashi M, Koumura T, Nonaka I, Hayashi YK, Noguchi S, Sher RB, Nakagawa Y, Manfredi G *et al*. (2011) Muscle choline kinase beta defect causes mitochondrial dysfunction and increased mitophagy. *Hum Mol Genet* **20**, 3841–3851.
52 Gallego-Ortega D, Ramirez de Molina A, Ramos MA, Valdes-Mora F, Barderas MG, Sarmentero-Estrada J & Lacal JC (2009) Differential role of human choline kinase alpha and beta enzymes in lipid metabolism: implications in cancer onset and treatment. *PLoS One* **4**, e7819.
53 Chua BT, Gallego-Ortega D, Ramirez de Molina A, Ullrich A, Lacal JC & Downward J (2009) Regulation of Akt(ser473) phosphorylation by choline kinase in breast carcinoma cells. *Mol Cancer* **8**, 131.
54 Nakai K & Horton P (1999) PSORT: a program for detecting sorting signals in proteins and predicting their subcellular localization. *Trends Biochem Sci* **24**, 34–36.
55 Larsson S, Ryden T, Holst U, Oredsson S & Johansson M (2008) Estimating the total rate of DNA replication using branching processes. *Bull Math Biol* **70**, 2177–2194.
56 Mori N, Glunde K, Takagi T, Raman V & Bhujwalla ZM (2007) Choline kinase down-regulation increases the effect of 5-fluorouracil in breast cancer cells. *Cancer Res* **67**, 11284–11290.
57 Dygas A & Baranska J (2001) Lipids and signal transduction in the nucleus. *Acta Biochim Pol* **48**, 541–549.
58 Hunt AN, Clark GT, Attard GS & Postle AD (2001) Highly saturated endonuclear phosphatidylcholine is synthesized *in situ* and colocated with CDP-choline pathway enzymes. *J Biol Chem* **276**, 8492–8499.
59 Irvine RF (2002) Nuclear lipid signaling. *Sci STKE* **2002**, RE13.
60 Cui Z, Houweling M, Chen MH, Record M, Chap H, Vance DE & Terce F (1996) A genetic defect in phosphatidylcholine biosynthesis triggers apoptosis in Chinese hamster ovary cells. *J Biol Chem* **271**, 14668–14671.
61 Terce F, Brun H & Vance DE (1994) Requirement of phosphatidylcholine for normal progression through the cell cycle in C3H/10T1/2 fibroblasts. *J Lipid Res* **35**, 2130–2142.

62 Yalcin A, Clem B, Makoni S, Clem A, Nelson K, Thornburg J, Siow D, Lane AN, Brock SE, Goswami U *et al*. (2010) Selective inhibition of choline kinase simultaneously attenuates MAPK and PI3K/AKT signaling. *Oncogene* **29**, 139–149.
63 Bradford MM (1976) A rapid and sensitive method for the quantitation of microgram quantities of protein utilizing the principle of protein-dye binding. *Anal Biochem* **72**, 248–254.
64 Osborn M, Debus E & Weber K (1984) Monoclonal antibodies specific for vimentin. *Eur J Cell Biol* **34**, 137–143.
65 Rober RA, Weber K & Osborn M (1989) Differential timing of nuclear lamin A/C expression in the various organs of the mouse embryo and the young animal: a developmental study. *Development* **105**, 365–378.
66 Harborth J, Elbashir SM, Bechert K, Tuschl T & Weber K (2001) Identification of essential genes in cultured mammalian cells using small interfering RNAs. *J Cell Sci* **114**, 4557–4565.
67 Schmittgen TD & Livak KJ (2008) Analyzing real-time PCR data by the comparative C(T) method. *Nat Protoc* **3**, 1101–1108.

Supporting information

The following supplementary material is available:
Fig. S1. Relative levels of total CKα, CKα2 and CKβ mRNAs in HeLa cells under different siRNA treatments were determined by quantitative real-time RT-PCR.
Fig. S2. Individual and double silencing of human CK isoforms in MCF-7 cells produce similar phenotype as in HeLa cells.
Fig. S3. HeLa cells transfected with siGL2 (negative control) showed normal mitotic spindles and displayed normal microtubular structure with no apoptosis after release from S-phase arrest.

This supplementary material can be found in the online version of this article.

Please note: As a service to our authors and readers, this journal provides supporting information supplied by the authors. Such materials are peer-reviewed and may be reorganized for online delivery, but are not copy-edited or typeset. Technical support issues arising from supporting information (other than missing files) should be addressed to the authors.